

PROCEEDINGS OF THE 1ST CANADA-US ROCK MECHANICS SYMPOSIUM, VANCOUVER,  
CANADA, 27-31 MAY 2007

# Rock Mechanics

## Meeting Society's Challenges and Demands

VOLUME 2: Case Histories

### *Editors*

Erik Eberhardt

*University of British Columbia, Vancouver, Canada*

Doug Stead

*Simon Fraser University, Burnaby, Canada*

Tom Morrison

*Greater Vancouver Regional District, Canada*



Taylor & Francis

Taylor & Francis Group

LONDON / LEIDEN / NEW YORK / PHILADELPHIA / SINGAPORE

## Table of contents

Preface	XIX
---------	-----

### VOLUME 1 – Fundamentals, New Technologies & New Ideas

#### *New Trends in Data Collection & 3-D Ground/Deformation Characterization*

Geology, technology and site characterisation <i>C.D. Martin</i>	3
Four dimensional considerations in forensic and predictive simulation of hazardous slope movement <i>D.J. Hutchinson, M.S. Diederichs, C. Carranza-Torres, R. Harrap, S. Rozic &amp; P. Graniero</i>	11
Integrated, real-time, 3D GIS-based geotechnical hazard assessment <i>J. McGaughey, R. McLeod &amp; G. Pears</i>	21
Application and limitations of ground-based laser scanning in rock slope characterization <i>M. Sturzenegger, M. Yan, D. Stead &amp; D. Elmo</i>	29
Comparison of terrestrial-based, high resolution, LiDAR and digital photogrammetry surveys of a rock slope <i>C.D. Martin, D.D. Tannant &amp; H. Lan</i>	37
A digital approach for integrating geotechnical data and stability analyses <i>H. Lan &amp; C.D. Martin</i>	45
The use of Slope Stability Radar (SSR) in managing slope instability hazards <i>N.J. Harries &amp; H. Roberts</i>	53
New insight techniques to analyze rock-slope relief using DEM and 3D-imaging cloud points: COLTOP-3D software <i>M. Jaboyedoff, R. Metzger, T. Oppikofer, R. Couture, M.-H. Derron, J. Locat &amp; D. Turmel</i>	61
High resolution 3D imaging for site characterisation of a nuclear waste repository <i>A. Gaich, M. Pötsch &amp; W. Schubert</i>	69
The application of metric 3D images for the mechanical analysis of keyblocks <i>M. Pötsch, W. Schubert &amp; A. Gaich</i>	77
Assessment of laser-based displacement mapping in an underground opening <i>F. Lemy, S. Yong &amp; T. Schulz</i>	85
Use of a 3-D scanning laser to quantify drift geometry and overbreak due to blast damage in underground manned entries <i>J. Warneke, J.G. Dwyer &amp; T. Orr</i>	93
Directional roughness profiles from three dimensional photogrammetric or laser scanner	

Joint set definition using topology based structure mapping <i>G.V. Poropat, M.K. Elmouttie &amp; D. Walford</i>	107
The surface expression of strain accumulation in failing rock masses <i>N.J. Rosser, D.N. Petley, S.A. Dunning, M. Lim &amp; S. Ball</i>	113
Predicting inter-well rock mechanics parameters using geophysical logs and 3-D seismic data <i>Y.G. Zhang, H.X. Han, M.B. Dusseault, X.J. Wang, Z.X. Zhang, K.M. Fan &amp; Y.M. Yu</i>	121
Geotechnical data management using acQuire workflows and data integrity <i>M.J. Murphy &amp; B.A. Murphy</i>	129
Characterising the in situ fragmentation of a fractured rock mass using a discrete fracture network approach <i>S.F. Rogers, D.K. Kennard, W.S. Dershowitz &amp; A. Van As</i>	137
3D simulation and aggregation of fracture network <i>M. Cravero, F. Piana, S. Ponti, S. Tallone &amp; G. Balestro</i>	145
Discrete fracture network modeling for carbonate rock <i>W.S. Dershowitz &amp; P.R. La Pointe</i>	153
Analysis of block removability in rock excavation by probabilistic approach <i>G. Chen, H. Li &amp; W. Zhou</i>	159
Accounting for local roughness in geostatistical simulation of fracture surface topography <i>H. Saito, G. Grasselli &amp; A.M. Ferrero</i>	167
 <i>Rock Mass Classification, Characterization &amp; Behaviour</i>	
Future directions for rock mass classification and characterization – Towards a cross-disciplinary approach <i>N. Barton</i>	179
Rock mass classification challenges <i>D. Milne</i>	191
Automatic drilling process monitoring (DPM) for in-situ characterization of weak rock mass strength with depth <i>Z.Q. Yue, J. Chen &amp; W. Gao</i>	199
RD <sub>i</sub> - A new method for evaluating of rock mass drillability <i>S.H. Hoseinie, M. Ataie, H. Aghababaei &amp; Y. Pourrahimian</i>	207
Rock slope design using slope stability rating (SSR) – Application and field verifications <i>A. Taheri &amp; K. Tani</i>	215
A new geomechanical evaluation system for slopes: SF <sub>i</sub> system <i>U. Jeong, W.S. Yoon, J. Park, B.H. Han, H-J. Park &amp; J.W. Choi</i>	223
Establishing a site specific mining geotechnical logging atlas <i>B.A. Murphy &amp; J.R. Campbell</i>	231
Rock mass strength with non-persistent joints <i>B.H. Kim, M. Cai &amp; P.K. Kaiser</i>	241

A modified approach for prediction of strength and post yield behaviour for high GSI rockmasses in strong, brittle ground <i>M.S. Diederichs, J.L. Carvalho &amp; T.G. Carter</i>	249
Peak and residual strengths of jointed rock masses and their determination for engineering design <i>M. Cai, P.K. Kaiser, Y. Tasaka &amp; M. Minami</i>	259
Characteristics and classification of New Zealand greywackes <i>S.A.L. Read &amp; L. Richards</i>	269
An approach for prediction of strength and post yield behaviour for rock masses of low intact strength <i>J.L. Carvalho, T.G. Carter &amp; M.S. Diederichs</i>	277
Deformation moduli of soft rocks in Japan through Geological Strength Index (GSI) <i>T. Yamamoto, K. Tsusaka &amp; C. Tanimoto</i>	287
Estimation of rock mass deformation modulus using the rock mass classifications and seismic measurements <i>H.R. Zarei, A. Uromeihy &amp; S. Khalesi</i>	297
Analysis of permeability using BPF, ANFIS & SOM <i>K. Shahriar &amp; H. Owladeghaffari</i>	303
 <i>Numerical Modelling – Continuum &amp; Discontinuum</i>	
Limit equilibrium, strength summation and strength reduction methods for assessing slope stability <i>J. Krahn</i>	311
Shear Strength Reduction (SSR) approach for slope stability analyses <i>M.S. Diederichs, M. Lato, R. Hammah &amp; P. Quinn</i>	319
Analysis of blocky rock slopes with finite element shear strength reduction analysis <i>R.E. Hammah, T. Yacoub, B. Corkum, F. Wibowo &amp; J.H. Curran</i>	329
Three-dimensional kinematic conditions for toppling <i>M.R. Yeung &amp; K.L. Wong</i>	335
A synthetic rock mass model for jointed rock <i>M. Pierce, P. Cundall, D. Potyondy &amp; D. Mas Ivars</i>	341
Investigating raise stability using fracture system and particle flow tools <i>J. Hadjigeorgiou, K. Esmaili &amp; M. Grenon</i>	351
Quantification of energy absorption capacity of trees against rockfall using finite element analysis <i>M.J. Jonsson, A. Volkwein &amp; W.J. Ammann</i>	359
Validation of a synthetic rock mass model using excavation induced microseismicity <i>J.M. Reyes-Montes, W.S. Pettitt &amp; R.P. Young</i>	365
Effect of dilation angle on failure process and mechanical behavior for a rock specimen with initial random material imperfections <i>V.D. ...</i>	371

DEM boundary conditions for modeling uniaxial and biaxial tests <i>D.D. Tannant &amp; C. Wang</i>	385
Compaction behavior of unbonded granular media: Discrete particle vs. experimental vs. analytical modeling <i>R.M. Holt, L. Li &amp; J.F. Stenebråten</i>	393
Effect of characteristic length in the finite element solution of elastic deformation of layered materials <i>A. Riahi &amp; J.H. Curran</i>	403
An equivalent continuum approach to coalmine water simulation <i>D.P. Adhikary &amp; H. Guo</i>	411
Long term tunnel stability in soft rock considering the influence of permeability using a coupled analysis <i>K. Kishida, T. Sakata, T. Hosoda, A. Tomita &amp; T. Adachi</i>	419
Three dimensional modelling of spiling bolts for tunnelling in a weakness zone <i>Q.N. Trinh, E. Broch &amp; M. Lu</i>	427
A finite element model for the stability analysis and optimum design of pressure tunnels <i>H. Ahmadi, A. Soltani &amp; A. Fahimifar</i>	433
Hydromechanical analysis of the effect of fracture properties on tunnel inflow <i>M. Sharifzadeh &amp; S. Karegar</i>	441
A model for coupled micro and macro-scale swelling processes in clay shales <i>M. Deriszadeh &amp; R.C.K. Wong</i>	447
 <i>Numerical Modelling – Brittle Fracture &amp; Damage</i>	
Simulation of multi-fracturing rock media including fluid/structure coupling <i>D.R.J. Owen, Y.T. Feng, M. Labao, C.R. Leonardi, S.Y. Zhao &amp; J. Yu</i>	457
Combined finite-discrete element modelling of surface subsidence associated with block caving mining <i>A. Vyazmensky, D. Elmo, D. Stead &amp; J.R. Rance</i>	467
Computational modeling of multiple fragmentation in rock masses with application to block caving <i>J.M. Rance, A. van As, D.R.J. Owen, Y.T. Feng &amp; R.J. Pine</i>	477
Methodology for estimation of excavation damaged zone around tunnels in hard rock <i>S.W. Shin, C.D. Martin, E.S. Park &amp; R. Christiansson</i>	485
Characterization of step-path failure mechanisms: A combined field based-numerical modeling study <i>M. Yan, D. Elmo &amp; D. Stead</i>	493
A discrete element damage model for rock slopes <i>A. Alzo'ubi, C.D. Martin &amp; D.M. Cruden</i>	503
PFC modeling of rock cutting under high pressure conditions <i>L.W. Ledgerwood III</i>	511
Numerical modeling of rock ridge breakage in rotary cutting <i>B. Yu &amp; A.W. Khair</i>	519

Fracture pattern of anisotropic rock by drilling or cutting using the PFC <i>N. Schormair &amp; K. Thuro</i>	527
A hydraulic fracture model with filtration for biosolids injection <i>G.W. Xia, M.B. Dusseault &amp; E. Marika</i>	535
 <i>Brittle Fracture &amp; Damage Mechanics</i>	
Effects of alteration on the engineering behaviour and intact rock fracture characteristics of granite under uniaxial compression <i>J.S. Coggan, J.L. Chilton, D. Stead, J.H. Howe &amp; R. Collins</i>	547
Crack initiation and propagation from frictional fractures <i>C.H. Park &amp; A. Bobet</i>	557
Crack growth study of a 3-D surface fracture under compression using strain and acoustic emission measurements <i>R.H.C. Wong, T.C. Li, K.T. Chau, S.C. Li &amp; W.S. Zhu</i>	565
Sliding crack model for the uniaxial compression of rock <i>E. David &amp; R.W. Zimmerman</i>	575
Coalescence behavior in Carrara marble and molded gypsum containing artificial flaw pairs under uniaxial compression <i>L.N.Y. Wong &amp; H.H. Einstein</i>	581
A fracture mechanics code for modelling sub-critical crack growth and time dependency <i>B. Shen &amp; M. Rinne</i>	591
Experimental study of subcritical crack growth in brittle materials <i>Y. Nara, M. Takada, K. Kaneko, H. Owada &amp; T. Hiraishi</i>	599
Subcritical crack growth of rocks using the double torsion method with consideration of the crack length <i>K.W. Kwok, R.H.C. Wong, K.T. Chau &amp; T.-f. Wong</i>	607
Experimental relationship between fracture toughness and fracture roughness in anisotropic granitic rocks <i>M.H.B. Nasser, G. Grasselli, B. Mohanty, J. Wirth &amp; M. Braun</i>	617
Effect of confining stress and loading rate on fracture toughness of rocks <i>T.Y. Ko &amp; J. Kemeny</i>	625
The evolution of fracture toughness and permeability in thermally cracked Westerly granite from elastic wave velocities <i>M.H.B. Nasser, R.P. Young &amp; A. Schubnel</i>	631
Fracture processes of rocks in dynamic tensile-splitting test <i>S.H. Cho, B. Mohanty, Y. Nakamura, Y. Ogata, H. Kitayama &amp; K. Kaneko</i>	639

Computerized Tomographic (CT) study of brittle material with internal flaw under hydraulic pressure and triaxial compression <i>W. Zhu, Y.S.H. Guo, S.C. Li, S.B. Li, N. Lee &amp; H. Jian</i>	661
Closure of hydraulic fractures visualized by X-ray CT technique in sand <i>Y. Dong &amp; C.J. de Pater</i>	665
 <i>In Situ Stress &amp; Stress Measurement</i>	
Is there a relation between the in situ principal stress magnitudes in rock masses? <i>J.P. Harrison, J.A. Hudson &amp; J.N. Carter</i>	675
In-situ stress estimation using crack closure energy in crystalline rock <i>S.S. Lim, C.D. Martin &amp; R. Christiansson</i>	683
A novel method for in situ stress measurement – concept, theory and numerical simulation <i>J.P. Loui, C-H. Ryu &amp; D-W. Ryu</i>	691
Interpretation of stressmeter data in variable temperature conditions <i>T. Smith, D. Milne &amp; Z. Szczepanik</i>	699
The contemporary stress field of the offshore Carnarvon Basin, North West Shelf, Western Australia <i>M.C. Neubauer, R.R. Hillis, R.C. King &amp; S.D. Reynolds</i>	705
Measurement of the regional and local stress field along a 10 km strike of the Zuleika Shear Zone in the Kundana gold mining province of Western Australia <i>C.R. Windsor, E. Villaescusa, T. Funatsu &amp; R. Lachenicht</i>	713
The measurement and interpretation of in-situ stress using an overcoring technique from surface <i>I. Gray &amp; L. See</i>	721
Evaluation of initial rock stress state by hydraulic fracturing test in Korea: Overall characteristics and a case study <i>S.H. Bae, J.M. Kim, J.S. Kim, E.S. Park &amp; S.W. Jeon</i>	729
 <i>Laboratory Testing &amp; Coupled Behaviour</i>	
Determination of aperture distribution and DNAPL migration in a rough-walled rock fracture <i>W.M.S.B. Weerakone &amp; R.C.K. Wong</i>	739
A laboratory study of grout flow and settlement in open fractures <i>B. Shen &amp; H. Guo</i>	747
Investigations on the swelling behavior of pure anhydrites <i>F. Rauh &amp; K. Thuro</i>	755
Shear testing of a model dam monolith under varying lateral constraint conditions <i>D. Galic, S.D. Glaser &amp; R.E. Goodman</i>	763
Time-dependant behavior of rock foundation by laboratory and numerical modeling in Gotvand Dam <i>M. Ahmadi, H.M.D. Niasar &amp; M.R. Bidgoli</i>	771
Shear failure and shear fracturing in shales <i>R. Nygård, M. Gutierrez &amp; K. Hoeg</i>	777
Influence of scale on the uniaxial compressive strength of brittle rock <i>L. Li, M. Aubertin, R. Simon, D. Deng &amp; D. Labrie</i>	785

The confining effect of end roughness on unconfined compressive strength <i>Z. Szczepanik, D. Milne &amp; C. Hawkes</i>	793
The long-term stress-strain behaviour of chalk <i>K.J.L. Stone &amp; K.I. Katsaros</i>	799
The effect of diagenesis on stress-strain behavior and acoustic velocities in sandstones <i>R. Nygård, K. Bjerlykke, K. Høeg &amp; G. Hareland</i>	805
The effective stress coefficient in porous sandstone <i>I.O. Ojala &amp; E. Fjær</i>	813
Development of upper and lower bounds to describe engineering properties as a function of macroporosity <i>A. DaCosta, C. Wright, Y. Ye, M. MacLaughlin &amp; N. Hudyma</i>	821
Determining abrasivity with the LCPC Test <i>K. Thuro, J. Singer, H. Käsling &amp; M. Bauer</i>	827
Weathering and geomechanical properties of Alvand granitic rocks, Western Iran <i>A. Shafiei, M. Heidari &amp; M.B. Dusseault</i>	835
Evaluation of the mechanical and physical properties of rock containing pyrite by leaching tests <i>I. Woo, J.G. Kim, G.H. Lee, H.J. Park &amp; J.G. Um</i>	843
Author index	847

## VOLUME 2 – Case Histories

### *Natural & Engineered Slopes*

The use of geological models for foundations on rock; ‘Test Section’ of the Sea to Sky Highway Upgrade, B.C. <i>P. Schlotfeldt &amp; M. Goldbach</i>	853
Estimating lateral support pressure for rock cuts at Washington-Dulles International Airport expansion <i>C.D. Martin, E.B. Rehwoldt &amp; V. Gall</i>	861
Dip slope analysis and parameter uncertainty – Case history and practical recommendations <i>B.R. Fisher &amp; E. Eberhardt</i>	871
Rockslope engineering challenges for power transmission lines, Las Vegas, Clark County, Nevada <i>W.C.B. Gates &amp; C. Lukkarila</i>	879
Rock fall hazard assessment of Chapmans Peak Drive, Cape Town, South Africa <i>P. Schlotfeldt</i>	887
Seismic monitoring of rockfall, Helmet Mountain, British Columbia <i>J.R. Moore, J.W. Sanders, K.M. Cuffey, J.R. Haught &amp; S.D. Glaser</i>	895
Deformation behavior of deep-seated rockslides in crystalline rock	901

A complex rock slope failure investigated by means of numerical modelling based on laser scanner technique <i>M. Ghirotti &amp; R. Genevois</i>	917
Ground-based and airborne LiDAR for structural mapping of the Frank Slide <i>M. Sturzenegger, D. Stead, C. Froese, F. Moreno &amp; M. Jaboyedoff</i>	925
Geomechanical analysis of the instability phenomena at Stromboli volcano <i>P. Tommasi, D. Boldini, F. Cignitti, A. Graziani, A. Lombardi &amp; T. Rotonda</i>	933
Characterization and back analysis of a complex slope deformation: San Bartolo Cliff <i>S. D'Ambra</i>	943
Affect of shear strength criteria selection in probabilistic rock slope stability analyses: A case study for a jointed rock slope in Norway <i>H.S.B. Düzgün &amp; R.K. Bhasin</i>	951
Dynamic rock fragmentation causes low rock-on-rock friction <i>T.R. Davies, M.J. McSaveney &amp; A.M. Deganutti</i>	959
Geotechnical challenges facing infrastructure development in western China <i>D.H. Zou, P. Cui &amp; Y.Y. Zhu</i>	967
Construction of a landslide susceptibility map using SINMAP technique and its validation: A case study <i>U. Jeong, S.I. Park, C.W. Lee, J-T. Lee, W.S. Yoon, J.W. Choi, H. Hong &amp; K.J. Kwan</i>	975
Stability analysis of the slope of debris-flow fan under artificial rainfall <i>Y.Y. Zhu, P. Cui &amp; D.H.S. Zou</i>	979
Probabilities of casualties on Al-Baha mountain road, Saudi Arabia <i>B.H. Sadagah</i>	987
Evaluating the slope instability of the Amiya slide <i>T.N. Singh &amp; A.K. Verma</i>	993
 <i>Dams &amp; Hydroelectric Projects</i>	
A hydroelectric utility client's view of rock engineering consultants <i>B.D. Ripley, D.P. Moore &amp; A.D. Watson</i>	1001
Estimating rock mass strength for a concrete dam founded on good rock: Blind Slough Dam, British Columbia, Canada <i>M.S. Lawrence &amp; C.D. Martin</i>	1007
Investigations and monitoring of rock slopes at Checkerboard Creek and Little Chief Slide <i>A.D. Watson, D.P. Moore, T.W. Stewart &amp; J.F. Psutka</i>	1015
Engineering geology, glacial preconditioning, and rockmass response to large scale underground excavations in the Niagara Region <i>M.A. Perras &amp; M.S. Diederichs</i>	1023
Geomechanics overview of large-scale hydropower station development in China <i>H.C. Zhu, N.C. Qi &amp; H.B. Wu</i>	1031
Accounting for time-dependent deformation in the Niagara Diversion Tunnel design <i>S.J. Rigbey &amp; M. Hughes</i>	1039

Hydraulic fracturing stress measurements in Iceland and the design of two hydroelectric power projects <i>B. Haimson &amp; A.K. Ingimarsson</i>	1047
Upgrading the rock foundation stability of Hamidieh Dam with relief wells <i>H.R. Zarei &amp; S. Khalesi</i>	1055
Rock mass characterization at the proposed Khorram-Roud dam site in western Iran <i>A. Shafiei, M. Heidari &amp; M.B. Dusseault</i>	1065
The effects of jet grouting on slope stability at Shahriar dam, Iran <i>B. Nikbakhtan, Y. Pourrahimian &amp; H. Aghababaei</i>	1075
 <i>Tunnels &amp; Deep Underground Excavations</i>	
Some opportunities for science and engineering at DUSEL <i>D. Elsworth &amp; C. Fairhurst</i>	1085
Construction of a large-deep permanent cavern for physics research at the Deep Underground Science and Engineering Laboratory (DUSEL) <i>C. Laughton</i>	1091
Towards a transparent Earth <i>S.D. Glaser, W. Roggenthen, L.R. Johnson &amp; E.L. Majer</i>	1097
Earth science collaborations for Deep Underground Science and Engineering Laboratory <i>J.S.Y. Wang</i>	1105
Investigating coupled mechanical-hydrological behavior in a DUSEL <i>H.F. Wang, S.C. Blair, S.R. Carlson, S.J. Martel &amp; T. Tokunaga</i>	1115
The 'Observational Approach' in tunnelling <i>W. Schubert</i>	1123
Geomechanical characterisation of massive rock for deep TBM tunnelling <i>M.C. Villeneuve, M.S. Diederichs, P.K. Kaiser &amp; C. Frenzel</i>	1131
Brittle tectonics in metamorphic rocks: Implications in the excavation of the Bodio Section of the Gotthard Base Tunnel <i>L. Bonzanigo</i>	1141
Methods for the evaluation and interpretation of displacement monitoring data in tunnelling <i>K. Grossauer &amp; W. Schubert</i>	1149
Rock classification based on convergence measurements in tunneling <i>C. Tanimoto, K. Tsusaka, Y. Mitarashi &amp; T. Aoki</i>	1157
Experience with shear zones at the edge of an intrusive body during tunnel construction <i>W. Steiner</i>	1167
Material behaviour associated with tunnelling through the weak rock masses of the	

Horonobe URL project – present status and future plans <i>H. Matsui, H. Kurikami, T. Kunimaru, H. Morioka &amp; K. Hatanaka</i>	1193
Application of scientific visualisation – stress control on permeability anisotropy in moderately fractured rock <i>L. Cotesta, P.K. Kaiser, M. Cai &amp; A. Vorauer</i>	1203
Rock mass yielding in the Äspö Pillar Stability Experiment <i>J.C. Andersson, R. Christiansson &amp; C.D. Martin</i>	1213
Design and operation of a pilot plant for underground LNG storage <i>E-S. Park, S-K. Chung, H-S. Lee, D-H. Lee &amp; H-Y. Kim</i>	1221
Numerical simulation evaluating the standoff distance of SPR caverns from the edge of the Big Hill Salt Dome, USA <i>B.Y. Park, C.G. Herrick, M.Y. Lee &amp; B.L. Ehgartner</i>	1227
 <i>Open Pit Mining</i>	
Predicting the behaviour and failure of large rock slopes <i>J.R.L. Read</i>	1237
Analysis of slope stability in strong, fractured rock at the Diavik Diamond Mine, NWT <i>K.M. Moffitt, S.F. Rogers, R.J. Beddoes &amp; S. Greer</i>	1245
Geotechnical study and optimum pit slope design of the Ashok Coal opencast project <i>V.K. Singh</i>	1251
Forecasting potential rock slope failure in open pit mines using the inverse-velocity method – Case examples <i>N.D. Rose &amp; O. Hungr</i>	1255
Footwall slope slab failure at a mountain coal mine <i>D.D. Tannant &amp; R. LeBreton</i>	1263
The application of resource modeling and GIS tools to establish the kinematic stability of rock slopes <i>M. Grenon, C. Lebleu, A.J. Laflamme &amp; M.A. Mostafavi</i>	1271
Geotechnical characterization and design for the transition from the Grasberg Open Pit to the Grasberg Block Cave mine <i>A. Srikant, C. Brannon, D.C. Flint &amp; T. Casten</i>	1277
A hybrid FEM/DEM approach to model the interaction between open-pit and underground block-caving mining <i>D. Elmo, A. Vyazmensky, D. Stead &amp; J.R. Rance</i>	1287
Use of resource modeling tools in numerical analysis of slope stability <i>M. Grenon &amp; R. Caumartin</i>	1295
Analysis of a rock slope failure in a limestone open pit <i>M. Cravero, G. Iabichino &amp; D. Lo Presti</i>	1301
 <i>Underground Mining</i>	
Geotechnical inputs for cave management in the DOZ block cave <i>H.A. Sahupala &amp; A. Srikant</i>	1313

Caving performance through integration of micro-seismic activity and numerical modeling at DOZ – PT Freeport Indonesia <i>E. Rubio &amp; D. Napitupulu</i>	1321
Modelling the caving of stope backs under high stress conditions: A case study of prediction and field trials <i>R.K. Brummer, C.P. O'Connor, G. Swan, D. Counter &amp; N. Disley</i>	1329
Numerical modeling analysis for São Bento Mineração S/A, Santa Bárbara, MG, Brazil <i>B. Foo &amp; R. Pakalnis</i>	1337
Stability assessment of non-entry stopes using nonlinear finite element analysis <i>Y. Zhang &amp; H.S. Mitri</i>	1347
Learning from ground failures – Underground mining case studies <i>J. Ran</i>	1353
Mining and rock mass factors influencing hangingwall dilution <i>K. Forster, D. Milne &amp; A. Pop</i>	1361
Mining within a weak rock mass – Kencana Underground Mine case study – PT Nusa Halmahera Minerals (Newcrest Mining Ltd), Indonesia <i>I. Febrian, A. Wahyudin, C. Gunadi, D. Peterson, P. Mah &amp; R. Pakalnis</i>	1367
Hazard assessment when mining orebodies under shear loading <i>F.T. Suorineni, P.K. Kaiser &amp; J. Delgado</i>	1377
Monitoring the behavior of a sill pillar at failure in a narrow-vein mine <i>D. Labrie, R. Boyle, T. Anderson, B. Conlon &amp; K. Judge</i>	1385
Estimation of the peak and post-peak behaviour of fractured rock masses using spatial and temporal analysis of mine induced microseismicity <i>A.L. Coulson, W.F. Bawden &amp; J.J. Crowder</i>	1395
Seismic hazard assessment and the amelioration thereof in deep level mining operations <i>S.K. Murphy &amp; G.F. Hoffmann</i>	1405
Coulomb Stress Triggering in the underground mining environment <i>G.F. Hofmann &amp; S.K. Murphy</i>	1415
Seismic monitoring in mines – Design, operation, tricks and traps <i>M.R. Hudyma &amp; R.K. Brummer</i>	1423
Back analysis and performance of Block A long hole open stopes – Kanowna Belle Gold Mine <i>P.M. Cepuritis, E. Villaescusa &amp; R. Lachenicht</i>	1431
Review of crown pillar investigations in a historic mine camp <i>J.G. Henning</i>	1441
Observations and evaluation of floor benching effects on pillar stability in U.S. limestone mines <i>G.S. Esterhuizen, D.R. Dolinar &amp; J.L. Ellenberger</i>	1447

Pillar stability during underground mining of the complete thickness of a thick coal seam in a single lift – Indian experiences <i>R. Singh &amp; R. Kumar</i>	1463
Geomechanical maintenance of flooded field mining problems <i>A. Grigoryev</i>	1469
Time-dependent rock mass behavior: Carr Fork Mine test stope <i>W.G. Pariseau</i>	1475
The application of computer mine modeling for wide room deep level potash mining in Saskatchewan <i>V. Ong, V. Thom, S. Munroe &amp; L. Suru</i>	1483
State of stress simulation during mining of salt in solution <i>V. Arad, S. Arad, P. Chelaru, I. Ilie, D. Ciocan &amp; D. Cotes</i>	1489
 <i>Rock Support, Ground Control &amp; Blasting</i>	
Evolution of ground support practices at Agnico-Eagle's LaRonde Division – Innovative solutions to high-stress yielding ground <i>F. Mercier-Langevin &amp; P. Turcotte</i>	1497
Numerical modeling and dynamic simulation of high-tensile steel wire mesh for ground support under rockburst loading <i>A. Roth, R. Ranta-Korpi, A. Volkwein &amp; C. Wendeler</i>	1505
Rock bolt characterization using guided waves and numerical simulation <i>D.H. Zou &amp; J.L. Cheng</i>	1511
Shear reinforcing effect of rust proofing expansive rock bolts <i>M. Shinji, H. Mukaiyama, N. Kanda &amp; H. Tanase</i>	1517
Reinforcement design of blocky rock masses with cable bolts in Discontinuous Deformation Analysis (DDA) algorithm <i>R. Grayeli</i>	1525
Modeling of shotcrete under ASTM C-1550 with PFC3D <i>X.J. Zhou &amp; R.L. McNearney</i>	1533
Inspection of rock-concrete interface in underground support systems using a Non-destructive Testing technique <i>Z. Hosseini, M. Momayez &amp; F. Hassani</i>	1541
Using blast vibration measurements to estimate rock triaxial strains/stresses and dynamic rock strength for blast damage evaluation <i>R. Yang &amp; D.S. Scovira</i>	1547
A strategy for increasing reliability of underground construction <i>B. Amusin</i>	1553
Investigation of overburden movement and a grout injection trial for mine subsidence control <i>H. Guo, B. Shen &amp; S. Chen</i>	1559
Case study review of rock mass response to artificial ground freezing <i>T.L.M. Smith, D. Milne &amp; C. Hawkes</i>	1567

Numerical modeling approach of failure modes for cemented backfill sill mats <i>C. Caceres, R. Pakalnis, P. Hughes &amp; T. Brady</i>	1575
Study of cemented rockfill for longhole stoping <i>M. Kockler &amp; S.J. Jung</i>	1581
Preliminary investigation into gel fill: Strength development and characteristics of sand paste fill with sodium silicate. <i>S.M. Razavi &amp; F. Hassani</i>	1585
 <i>Petroleum Resources &amp; Borehole Geomechanics</i>	
Geomechanical characterization of the Weyburn Field for geological storage of CO <sub>2</sub> <i>R.J. Chalaturnyk</i>	1595
Some fundamental aspects of reservoir and crustal permeability and strength <i>N. Barton</i>	1601
Predicting the stress changes induced by fluid production and injection in porous reservoirs <i>H. Soltanzadeh &amp; C.D. Hawkes</i>	1609
Stress field in the vicinity of a natural fault activated by the propagation of an induced hydraulic fracture <i>M. Thiercelin &amp; E. Makkhyu</i>	1617
A semi-analytical model for predicting fault reactivation tendency induced by pore pressure change <i>H. Soltanzadeh &amp; C.D. Hawkes</i>	1625
Hydraulic fracturing of oil reservoirs in water-sensitive tuff <i>H.X. Han, M.B. Dusseault, X.J. Wang, P.F. Tang, H. Zhang &amp; X.W. Deng</i>	1633
Hydraulic fracture propagation across frictional interfaces <i>X. Zhang &amp; R.G. Jeffrey</i>	1639
Viscosity-dominated hydraulic fractures <i>E. Detournay, A.P. Peirce &amp; A.P. Bunger</i>	1649
Porothermoelastic analysis of wellbore failure and determination of in situ stress and rock strength <i>Q. Tao &amp; A. Ghassemi</i>	1657
Cyclic loading of oil sand by large mobile mining equipment <i>T.G. Joseph &amp; A.D. Sharif-Abadi</i>	1665
Microseismic detection of casing failures at a heavy oil operation <i>S. Talebi, M. Coté &amp; R.J. Smith</i>	1671
Impact of rock properties on the relationship between wellbore breakout width and depth <i>D. Moos, S. Willson &amp; C.A. Barton</i>	1677
Impermeable drilling mud to strengthen wellbore stability <i>J. Zhang &amp; W.B. Standifird</i>	1685
Theoretical analysis of a shale ball subjected to chemoporomechanical loading <i>A.P. Bunger</i>	1691

Rock mechanical aspects of shaped charge penetration <i>J. Heiland, B. Grove &amp; I.C. Walton</i>	1711
Calculating unconfined rock strength from drilling data <i>G. Hareland &amp; R. Nygaard</i>	1717
Author index	1725

## Author index

- Adachi, T. 419  
Adhikary, D.P. 411  
Aghababaei, H. 207, 1075  
Ahmadi, H. 433  
Ahmadi, M. 771  
Alzo'ubi, A. 503  
Ammann, W.J. 359  
Amusin, B. 1553  
Anderson, T. 1385  
Andersson, J.C. 1213  
Anegg, J. 901  
Aoki, T. 1157  
Arad, S. 1489  
Arad, V. 1489  
Archambault, G. 379  
Ataie, M. 207  
Aubertin, M. 785
- Bae, S.H. 729  
Balestro, G. 145  
Ball, S. 113  
Bangaru, N.V. 647  
Barthélémy, J.F. 655  
Barton, C.A. 1677  
Barton, N. 179, 1601  
Bauer, M. 827  
Bawden, W.F. 1395  
Beddoes, R.J. 1245  
Bhasin, R.K. 951  
Bidgoli, M.R. 771  
Bjørlykke, K. 805  
Blair, S.C. 1115  
Block, G.I. 647  
Bobet, A. 557  
Boldini, D. 933  
Bonzanigo, L. 1141  
Boyle, R. 1385  
Brady, T. 1575  
Brannon, C. 1277  
Braun, M. 617  
Broch, E. 427  
Brummer, R.K. 1329, 1423  
Bunger, A.P. 1649, 1691
- Caceres, C. 1575  
Cai, M. 241, 259, 1203  
Campbell, J.R. 231  
Carlson, S.R. 1115
- Carvalho, J.L. 249, 277  
Casten, T. 1277  
Caumartin, R. 1295  
Cepuritis, P.M. 1431  
Chalaturnyk, R.J. 1595  
Chau, K.T. 565, 607  
Chelaru, P. 1489  
Chen, G. 159  
Chen, J. 199  
Chen, S. 1559  
Cheng, J.L. 1511  
Chilton, J.L. 547  
Cho, S.H. 639  
Choi, J.W. 223, 975  
Christiansson, R. 485, 683, 1213  
Chung, H.I. 1187  
Chung, S.-K. 1221  
Cignitti, F. 933  
Ciocan, D. 1489  
Coggan, J.S. 547  
Collins, R. 547  
Conlon, B. 1385  
Corkum, B. 329  
Cotes, D. 1489  
Cotesta, L. 1203  
Coté, M. 1671  
Coulson, A.L. 1395  
Counter, D. 1329  
Couture, R. 61  
Cravero, M. 145, 1301  
Crowder, J.J. 1395  
Cruden, D.M. 503  
Cuffey, K.M. 895  
Cui, P. 967, 979  
Cundall, P. 341  
Curran, J.H. 329, 403
- DaCosta, A. 821  
David, E. 575  
Davies, T.R. 959  
de Pater, C.J. 665  
Deganutti, A.M. 959  
Delgado, J. 1377  
Deng, D. 785  
Deng, X.W. 1633  
Deriszadeh, M. 447  
Derron, M.-H. 61
- Disley, N. 1329  
Dolinar, D.R. 1447  
Dong, Y. 665  
Dunning, S.A. 113  
Dusseault, M.B. 121, 535, 835, 1065, 1633, 1701  
Dwyer, J.G. 93  
D'Ambra, S. 943  
Düzgün, H.S.B. 951
- Eberhardt, E. 871, 901, 909  
Ehgartner, B.L. 1227  
Einstein, H.H. 581  
Ellenberger, J.L. 1447  
Elmo, D. 29, 467, 493, 1287  
Elmouttie, M.K. 107  
Elsworth, D. 1085  
Esmaili, K. 351  
Esterhuizen, G.S. 1447
- Fahimifar, A. 433  
Fairhurst, C. 1085  
Fan, K.M. 121  
Febrian, I. 1367  
Feng, Y.T. 457, 477  
Ferrero, A.M. 167  
Fisher, B.R. 871  
Fjær, E. 813  
Flint, D.C. 1277  
Foo, B. 1337  
Forster, K. 1361  
Frenzel, C. 1131  
Froese, C. 925  
Funatsu, T. 713
- Gaich, A. 69, 77  
Galic, D. 763  
Gall, V. 861  
Gao, W. 199  
Gates, W.C.B. 879  
Genevois, R. 917  
Ghassemi, A. 1657  
Ghirotti, M. 917  
Glaser, S.D. 763, 895, 1097  
Goldbach, M. 853  
Goodman, R.E. 763  
Graniero, P. 11  
Grasselli, G. 167, 617

- Grenon, M. 351, 1271, 1295  
 Grigoryev, A. 1469  
 Grossauer, K. 1149  
 Grove, B. 1711  
 Gunadi, C. 1367  
 Guo, H. 411, 747, 1559  
 Guo, Y.S.H. 661  
 Gupta, V. 647  
 Gutierrez, M. 777
- Hadjigeorgiou, J. 351  
 Haimson, B. 1047  
 Hammah, R. 319  
 Hammah, R.E. 329  
 Han, B.H. 223  
 Han, H.X. 121, 1633  
 Haneberg, W.C. 101  
 Harelund, G. 805, 1717  
 Harrap, R. 11  
 Harries, N.J. 53  
 Harrison, J.P. 675  
 Hassani, F. 1541, 1585  
 Hatanaka, K. 1193  
 Haught, J.R. 895  
 Hawkes, C. 793, 1567  
 Hawkes, C.D. 1609, 1625  
 Heidari, M. 835, 1065  
 Heiland, J. 1711  
 Henning, J.G. 1441  
 Hermanns, R.L. 909  
 Herrick, C.G. 1227  
 Hillis, R.R. 705  
 Hiraishi, T. 599  
 Hoffmann, G.F. 1405  
 Hofmann, G.F. 1415  
 Holt, R.M. 393  
 Hong, H. 975  
 Hoseinie, S.H. 207  
 Hosoda, T. 419  
 Hosseini, Z. 1541  
 Howe, J.H. 547  
 Hudson, J.A. 675  
 Hudyma, M.R. 1423  
 Hudyma, N. 821  
 Hughes, M. 1039  
 Hughes, P. 1575  
 Hungr, O. 1255  
 Hutchinson, D.J. 11  
 Høeg, K. 777, 805
- Iabichino, G. 1301  
 Ilie, I. 1489  
 Ingimarsson, A.K. 1047
- Jaboyedoff, M. 61, 925  
 Jeannin, L. 655  
 Jeffrey, R.G. 1639
- Jeon, S.W. 729  
 Jeong, U. 223, 975  
 Jian, H. 661  
 Johnson, L.R. 1097  
 Jonsson, M.J. 359  
 Joseph, T.G. 1665  
 Judge, K. 1385  
 Jun, H.J. 647  
 Jung, S.J. 1581
- Kaiser, P.K. 241, 259, 1131,  
 1203, 1377  
 Kanda, N. 1517  
 Kaneko, K. 599, 639  
 Karegar, S. 441  
 Katsaros, K.I. 799  
 Kemeny, J. 625  
 Kennard, D.K. 137  
 Khair, A.W. 519  
 Khalesi, S. 297, 1055  
 Kim, B.H. 241  
 Kim, H-Y. 1221  
 Kim, J.G. 843  
 Kim, J.M. 729  
 Kim, J.S. 729  
 King, R.C. 705  
 Kishida, K. 419  
 Kitayama, H. 639  
 Ko, T.Y. 625  
 Kockler, M. 1581  
 Krahn, J. 311  
 Kumar, R. 1463  
 Kunimaru, T. 1193  
 Kurikami, H. 1193  
 Kwan, K.J. 975  
 Kwok, K.W. 607  
 Kwon, Y.W. 1187  
 Käsling, H. 827
- La Pointe, P.R. 153  
 Labao, M. 457  
 Labrie, D. 785, 1385  
 Lachenicht, R. 713, 1431  
 Laflamme, A.J. 1271  
 Lan, H. 37, 45  
 Lato, M. 319  
 Loughton, C. 1091  
 Lawrence, M.S. 1007  
 Lebleu, C. 1271  
 LeBreton, R. 1263  
 Ledgerwood III, L.W. 511  
 Lee, C.W. 975  
 Lee, D-H. 1221  
 Lee, G.H. 843  
 Lee, H-S. 1221  
 Lee, J-T. 975  
 Lee, M.Y. 1227
- Lee, N. 661  
 Lee, Y.S. 1187  
 Lemy, F. 85  
 Leonardi, C.R. 457  
 Li, H. 159  
 Li, L. 393, 785  
 Li, S.B. 661  
 Li, S.C. 565, 661  
 Li, T.C. 565  
 Lim, M. 113  
 Lim, S.S. 683  
 Lo Presti, D. 1301  
 Locat, J. 61  
 Lombardi, A. 933  
 Loui, J.P. 691  
 Lu, M. 427  
 Lukkarila, C. 879
- MacLaughlin, M. 821  
 Mah, P. 1367  
 Majer, E.L. 1097  
 Makkhyu, E. 1617  
 Marika, E. 535  
 Marmier, R. 655  
 Martel, S.J. 1115  
 Martin, C.D. 3, 37, 45, 485, 503,  
 683, 861, 1007, 1213  
 Mas Ivars, D. 341  
 Matsui, H. 1193  
 McGaughey, J. 21  
 McIntire, H. 1455  
 McLeod, R. 21  
 McNearny, R.L. 1533  
 McSaveney, M.J. 959  
 Mercier-Langevin, F. 1497  
 Metzger, R. 61  
 Milne, D. 191, 699, 793, 1361,  
 1567  
 Minami, M. 259  
 Mitarashi, Y. 1157  
 Mitri, H.S. 1347  
 Moffitt, K.M. 1245  
 Mohanty, B. 617, 639  
 Momayez, M. 1541  
 Moore, D.P. 1001, 1015  
 Moore, J.R. 895  
 Moos, D. 1677  
 Moreno, F. 925  
 Morioka, H. 1193  
 Mostafavi, M.A. 1271  
 Mukaiyama, H. 1517  
 Munroe, S. 1483  
 Murphy, B.A. 129, 231  
 Murphy, M.J. 129  
 Murphy, S.K. 1405, 1415
- Nakamura, Y. 639  
 Napitupulu, D. 1321

- Nara, Y. 599  
 Nasseri, M.H.B. 617, 631  
 Neubauer, M.C. 705  
 Niasar, H.M.D. 771  
 Nikbakhtan, B. 1075  
 Noël, J.-F. 379  
 Nygård, R. 777, 805
- Ogata, Y. 639  
 Ojala, I.O. 813  
 Ong, V. 1483  
 Oppikofer, T. 61  
 Orr, T. 93  
 Owada, H. 599  
 Owen, D.R.J. 457, 477  
 Owladeghaffari, H. 303  
 O'Connor, C.P. 1329
- Pakalnis, R. 1337, 1367, 1575  
 Pariseau, W.G. 1475  
 Park, B.Y. 1227  
 Park, C.H. 557  
 Park, E.-S. 1221  
 Park, E.S. 485, 729  
 Park, H.-J. 223  
 Park, H.J. 843  
 Park, J. 223  
 Park, S.I. 975  
 Pears, G. 21  
 Peirce, A.P. 1649  
 Perras, M.A. 1023  
 Peterson, D. 1367  
 Petley, D.N. 113  
 Pettitt, W.S. 365  
 Piana, F. 145  
 Pierce, M. 341  
 Pine, R.J. 477  
 Ponti, S. 145  
 Pop, A. 1361  
 Poropat, G.V. 107  
 Potyondy, D. 341  
 Pourrahimian, Y. 207, 1075  
 Psutka, J.F. 1015  
 Pötsch, M. 69, 77
- Qi, N.C. 1031  
 Quinn, P. 319
- Ran, J. 1353  
 Rance, J.M. 477  
 Rance, J.R. 467, 1287  
 Ranta-Korpi, R. 1505  
 Rauh, F. 755  
 Razavi, S.M. 1585  
 Reed, J.R. 1227
- Reynolds, S.D. 705  
 Riahi, A. 403  
 Richards, L. 269  
 Rigbey, S.J. 1039  
 Rinne, M. 591  
 Ripley, B.D. 1001  
 Roberts, D. 1455  
 Roberts, H. 53  
 Rogers, S.F. 137, 1245  
 Roggenthen, W. 1097  
 Rose, N.D. 1255  
 Rosser, N.J. 113  
 Roth, A. 1505  
 Rothenburg, L. 1701  
 Rotonda, T. 933  
 Rozic, S. 11  
 Rubio, E. 1321  
 Ryu, C.-H. 691  
 Ryu, D.-W. 691
- Sadagah, B.H. 987  
 Sahupala, H.A. 1313  
 Saito, H. 167  
 Sakata, T. 419  
 Sanders, J.W. 895  
 Schlotfeldt, P. 853, 887  
 Schormair, N. 527  
 Schubert, W. 69, 77, 1123, 1149  
 Schubnel, A. 631  
 Schulz, T. 85  
 Schönlaub, H. 901  
 Scovira, D.S. 1547  
 See, L. 721  
 Shafiei, A. 835, 1065  
 Shahriar, K. 303  
 Sharif-Abadi, A.D. 1665  
 Sharifzadeh, M. 441  
 Shen, B. 591, 747, 1559  
 Shin, S.W. 485  
 Shinji, M. 1517  
 Simon, R. 785  
 Singer, J. 827  
 Singh, R. 1463  
 Singh, T.N. 993  
 Singh, V.K. 1251  
 Smith, R.J. 1671  
 Smith, T. 699  
 Smith, T.L.M. 1567  
 Soltani, A. 433  
 Soltanzadeh, H. 1609, 1625  
 Srikant, A. 1277, 1313  
 Standifird, W.B. 1685  
 Stead, D. 29, 467, 493, 547, 925,
- Stone, K.J.L. 799  
 Sturzenegger, M. 29, 925  
 Suorineni, F.T. 1377  
 Suru, L. 1483  
 Swan, G. 1329  
 Szczepanik, Z. 699, 793
- Taheri, A. 215  
 Takada, M. 599  
 Talebi, S. 1671  
 Tallone, S. 145  
 Tanase, H. 1517  
 Tang, P.F. 1633  
 Tani, K. 215  
 Tanimoto, C. 287, 1157  
 Tannant, D.D. 37, 385, 1263  
 Tao, Q. 1657  
 Tasaka, Y. 259  
 Thiercelin, M. 1617  
 Thom, V. 1483  
 Thuro, K. 527, 755, 827  
 Tokunaga, T. 1115  
 Tolfree, D. 1455  
 Tomita, A. 419  
 Tommasi, P. 933  
 Trinh, Q.N. 427  
 Tsusaka, K. 287, 1157  
 Turcotte, P. 1497  
 Turmel, D. 61
- Um, J.G. 843  
 Uromeihy, A. 297
- Van As, A. 137  
 van As, A. 477  
 Verma, A.K. 993  
 Villaescusa, E. 713, 1431  
 Villeneuve, M.C. 1131  
 Vlachopoulos, N. 1179  
 Volkwein, A. 359, 1505  
 Vorauer, A. 1203  
 Vyazmensky, A. 467, 1287
- Wahyudin, A. 1367  
 Walford, D. 107  
 Walton, I.C. 1711  
 Wang, C. 385  
 Wang, H.F. 1115  
 Wang, J.S.Y. 1105  
 Wang, X.B. 371  
 Wang, X.J. 121, 1633  
 Warneke, J. 93  
 Watson, A.D. 1001, 1015

Willson, S. 1677  
Windsor, C.R. 713  
Wirth, J. 617  
Wong, K.L. 335  
Wong, L.N.Y. 581  
Wong, R.C.K. 447, 739  
Wong, R.H.C. 565, 607  
Wong, T.-f. 607  
Woo, I. 843  
Wright, C. 821  
Wu, H.B. 1031

Xia, G.W. 535

Yacoub, T. 329  
Yamamoto, T. 287

Yan, M. 29, 493  
Yang, R. 1547  
Ye, Y. 821  
Yeung, M.R. 335  
Yin, S. 1701  
Yong, S. 85  
Yoon, W.S. 223, 975  
Young, R.P. 365, 631  
Yu, B. 519  
Yu, J. 457, 1187  
Yu, Y.M. 121  
Yue, Z.Q. 199

Zangerl, C. 901  
Zarei, H.R. 297, 1055  
Zhang, H. 1633

Zhang, J. 1685  
Zhang, X. 1639  
Zhang, Y. 1347  
Zhang, Y.G. 121  
Zhang, Z.X. 121  
Zhao, S.Y. 457  
Zhou, W. 159  
Zhou, X.J. 1533  
Zhu, H.C. 1031  
Zhu, W. 661  
Zhu, W.S. 565  
Zhu, Y.-Y. 979  
Zhu, Y.Y. 967  
Zimmerman, R.W. 575  
Zou, D.H. 967, 1511  
Zou, D.H.S. 979

**Minoski, Suzanne S. (CDC/NIOSH/PRL)**

---

**To:** Calhoun, Roberta A. (CDC/NIOSH/PRL); Bennett, William D. (Bill) (CDC/NIOSH/EID)  
**Cc:** Minoski, Suzanne S. (CDC/NIOSH/PRL)  
**Subject:** FW: Conference Proceedings #3435  
**Attachments:** 1170279846-CONFNL--2-.pdf

Bill,

I will be sending you the cover page and index for this one.

Thanks,  
Sue

---

**From:** Tuchman, Robert J. (CDC/CCHIS/NCHM)  
**Sent:** Monday, July 23, 2007 1:10 PM  
**To:** Minoski, Suzanne S. (CDC/NIOSH/PRL)  
**Subject:** RE: Conference Proceedings #3435

Esterhuizen GS, Dolinar DR, Ellenberger JL [2007]. Observations and evaluation of floor benching effects on pillar stability in U.S. limestone mines. In: Eberhardt E, Stead D, Morrison T, eds. Proceedings of the First Canada-U.S. Rock Mechanics Symposium (Vancouver, British Columbia, Canada, May 27–31, 2007). Taylor & Francis Ltd., 7 pp.



1170279846-CONF  
FNL--2-.pdf (88...

ADMIN CODE: HCCBJ  
CAN No: 7927Z04K

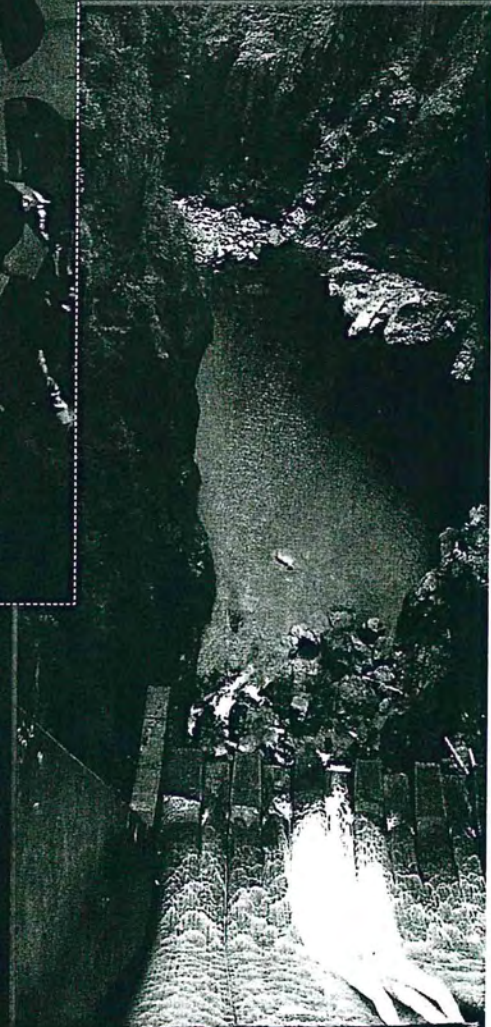
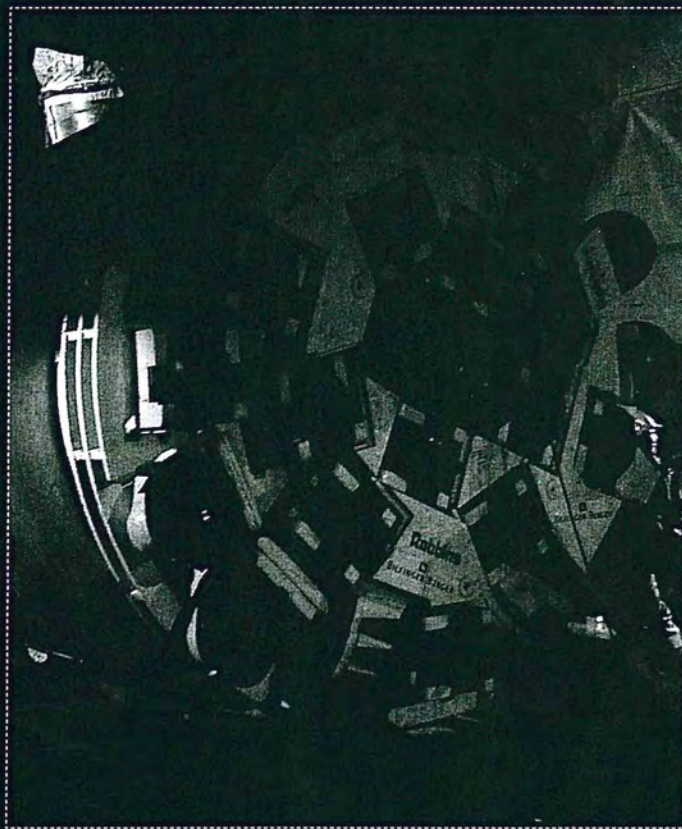
# Rock Mechanics

Meeting Society's Challenges and Demands

VOLUME 2: CASE HISTORIES

Editors

Erik Eberhardt  
Doug Stead  
Tom Morrison



 Taylor & Francis  
Taylor & Francis Group

# Observations and evaluation of floor benching effects on pillar stability in U.S. limestone mines

G.S. Esterhuizen, D.R. Dolinar & J.L. Ellenberger.

*National Institute for Occupational Safety and Health, Pittsburgh, USA.*

**ABSTRACT:** A survey of roof and pillar conditions in underground limestone mines in the United States has revealed that bench mining of the floor between pillars can cause instability in the pillars at the perimeter of the benched area. Increased loading of these pillars was observed at several mines. Large inclined geological structures that are exposed in pillar ribs were observed to contribute to pillar instability. The paper describes a study that was carried out using numerical models to assess the effects of bench mining on pillar load and stability. It was found that the benched pillars shed load onto the surrounding pillars owing to their reduced stiffness. The pillars at the perimeter of the benching area will start shedding load as soon as benching increases the height of one side of the pillar. A case study is described which shows the effects of bench mining on limestone mine pillars.

## 1 INTRODUCTION

Underground limestone mines in the U.S. make use of the room and pillar method of mining. Bench mining of the floor between the pillars is sometimes carried out to improve utilization of the reserves. Figure 1 shows an area where bench mining of the floor is underway. The benched pillars are in the foreground and the original development pillars are seen in the background. The National Institute for Occupational Safety and Health (NIOSH), Pittsburgh Research Laboratory is investigating pillar and roof stability in U.S. limestone mines. Observations of pillar conditions carried out as part of this study revealed that the condition of pillars around the perimeter of bench mining operations can be worse than elsewhere in the mine. Unstable pillar ribs represent a rock fall hazard to mine personnel. Over the decade from 1996 through 2005, ground falls were the cause of 36% of fatalities and 12% of all injury related lost workdays in underground limestone mines (Mine Safety and Health Administration, 2006). In addition, failure of a single pillar can result in overloading of the adjacent pillars, possibly resulting in the collapse of multiple pillars.

A total of 31 different mine sites were visited by NIOSH researchers. Bench mining of the floor had been carried out at 18 of the 31 mine sites visited. Evidence of increased instability of the pillars at or near the perimeter of the benched areas was observed at six of these mines. The observed instability was in the form of failure along pre-

existing geological structures and stress related spalling and fracturing of the pillar ribs.



Figure 1. Example of bench mining of the floor between pillars in a limestone mine.

This paper presents a summary of the observations made and the results of numerical analyses that were carried out to evaluate the changes in loading and pillar strength that occur during bench mining. A case study of pillar instability associated with bench mining is presented. The paper concludes with suggestions for identifying situations that are likely to result in instability during bench mining and strategies to limit the potential for instability.

## 2 FIELD OBSERVATIONS OF BENCH MINING IN LIMESTONE MINES

Field data on roof and pillar conditions were collected at 86 different locations in 31 limestone mines in Pennsylvania, Virginia, West Virginia, Illinois, Kentucky, Tennessee, Missouri and Indiana. The data collected at each location included rock mass properties, pillar and room dimensions, information on roof and pillar stability and rock strength properties, (Esterhuizen et al. 2006). The rock mass in these limestone mines can be classified as "Good" to "Very Good" with rock mass rating (RMR) values in the range of 70-85 units, using the Bieniawski (1989) method of classification. The intact rock strength is in the range of 100-200 MPa. Table 1 presents a summary of the dimensions of pillars and rooms showing both development and benching dimensions at the 31 mines. It can be seen that bench mining increases the average pillar height from 7.8 to 17.8 m and reduces the average the width-to-height (W:H) ratio of the pillars from 1.67 to 0.95.

Table 1. Dimensions of room-and-pillar mining layouts.

Parameter	Average	Minimum	Maximum
			m
Pillar height: development (m)	7.8	4.8	10.7
Pillar height: benched pillar (m)	17.8	9.9	38.0
Pillar width (m)	13.9	5.1	28.6
Pillar W:H: development	1.67	0.93	3.52
Pillar W:H: benched pillar	0.95	0.29	2.35
Room width (m)	13.5	9.1	16.8
Depth of cover (m)	121	23	533
Local percent extraction (%)	73	54	88

Observations of pillar conditions at the mines revealed several instances where the partially benched pillars at the edge of the benching operations had become unstable. Table 2 summarizes the cases in which pillar instability

Table 2. Summary of observed pillar instability associated with bench mining.

Case	W:H Develop	W:H Benched	Average Pillar stress (MPa)	Instability Observed
1	1.3	0.59	13.1	Large discontinuities exposed by benching, evidence of high horizontal stress, diagonal shearing through pillar. Benching was halted.
2	1.5	0.73	14.1	Progressive spalling of pillar ribs, pillar width reduced significantly, weak bedding infill contributed to spalling.
3	1.5	0.44	15.0	Spalling of several pillars to hourglass shape. Sloughing from one of the pillars caused by a large steeply dipping discontinuity.
4	1.65	0.61	8.14	Sloughing from pillar ribs as a large discontinuity is exposed at the perimeter of benching.
5	2.0	0.99	19.8	Sloughing from pillar walls at location of a large discontinuity. Benching was halted and resumed beyond this area.
6	1.96	0.92	13.1	Spalling to hourglass shape. Benching halted owing to presence of large discontinuities in adjacent pillars.

associated with bench mining was observed. Case 3 was evaluated in greater detail and is presented as a case study. Benching operations were halted in two of the observed cases owing to instability of the partially benched pillars. Several cases were observed in which the pillars at the perimeter of the benching area showed signs of increased loading. In addition, instability was observed when bench mining exposed large joint structures in the pillar ribs.

It was apparent from the field observations that benching not only reduces the pillar strength by increasing the pillar height, but also causes an increase in pillar load at the perimeter of the benched area. The increased pillar load can be ascribed to the fact that the benched pillars are taller and are consequently less stiff than the surrounding development pillars. Stresses are concentrated in the stiffer development pillars, which can result in instability in these pillars.

The average pillar stress shown in the table was calculated using the tributary area method, which does not account for increased loading owing to the variable stiffness of the benched and development pillars. Numerical model analyses were conducted to further quantify the load and strength changes caused by benching and evaluate their impact on pillar stability.

## 3 NUMERICAL ANALYSIS OF THE EFFECT OF BENCHING ON PILLAR STRENGTH AND LOADING

The summary of mining dimensions in Table 1 shows that the average width-to-height (W:H) ratio of pillars is reduced by 43% during benching operations. The effect of the increased height on pillar strength can be estimated using one of the published pillar strength equations for hard rock mines, such as the equation developed by Hedley

and Grant (1972). However, during benching, the height of a pillar is progressively increased as each side is benched, until all four sides are fully benched. The strength of a pillar during these stages of bench mining cannot be determined using existing pillar strength equations since the equations are intended for prism shaped pillars that have equal height on all sides. Numerical models were therefore used to estimate the strength of the irregular shaped pillars formed during benching. Figure 2 shows conceptually the stages of benching around a limestone pillar that were considered in the models. During Stage 1 one side of the pillar has been bench mined. At Stage 2, two sides have been benched and so on, until the pillar is fully benched in Stage 4. Numerical models were also used to investigate the

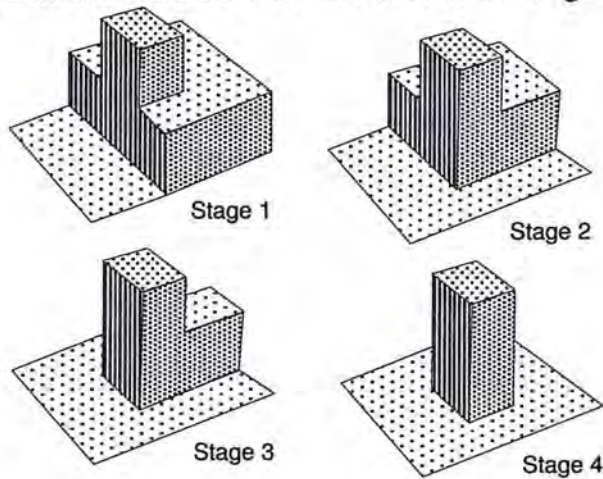


Figure 2. Stages of bench mining around a pillar considered in the numerical models.

changes in average pillar stress at each stage of bench mining.

### 3.1 Analysis of the Strength of Partially Benched Pillars

The progressive reduction in pillar strength during bench mining was assessed using the FLAC3D finite difference program (Anon, 2005). Models were set up to simulate square pillars with initial W:H ratios of 1.0 and 1.5. The benching stages shown in Figure 2 were modeled by progressively removing the floor rocks on each side of a pillar until it is fully benched on all sides. The benching depth was selected so that the pillar height was doubled during the benching procedure. The model geometry for the pillar with initial W:H = 1.0 is shown in Figure 3. Model element sizes were kept constant during all the runs to avoid element size effects on the results.

The mechanical properties that were used to simulate the limestone rock mass are summarized in Table 3. The properties were selected to model a rock mass with an RMR value of 70 and intact rock strength of 120 MPa. A bi-linear peak strength criterion with strain softening of the failed rock was used to capture both brittle spalling and shear failure

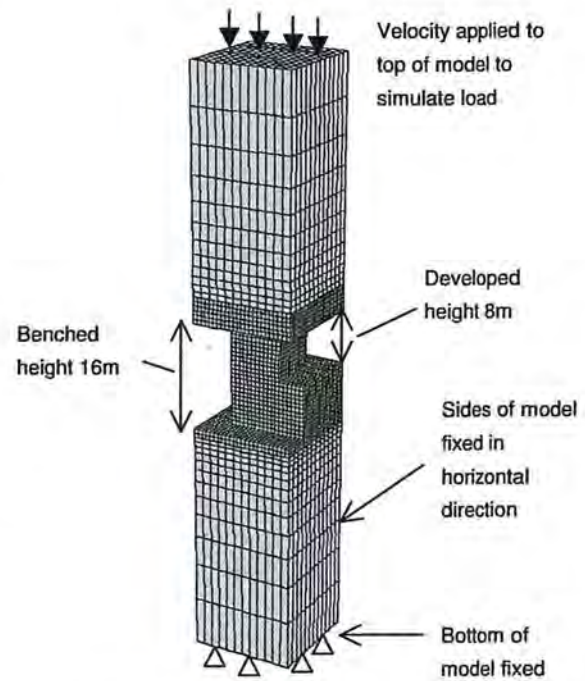


Figure 3. FLAC3D model of a partially benched pillar

Table 3. Input Parameters for the bilinear strength model.

Parameter	Value
Elastic modulus	70 GPa
Poisson ratio	0.2
Intact rock strength (UCS)	120 MPa
First stage (brittle) cohesion	20 MPa
First stage (brittle) friction angle	0°
Second stage cohesion	6.5 MPa
Second stage friction angle	42.7°
Tensile strength	7 MPa
Dilation angle	30°

of the limestone, as suggested by Kaiser et al. (2000), Martin & Maybee (2000) Diederichs (2002) and Diederichs et al. (2002). The brittle rock strength was set at 33% of the intact rock strength and the Coulomb strength properties of the rock mass were based on the Hoek-Brown (1997) criterion. Details of the modeling approach and selection of input parameters for this model are presented in Esterhuizen, (2006).

The strength of the modeled pillars was determined by gradually increasing the vertical load in the models. Failure of the rock in the models was allowed to occur in response to the increased loading. The loading was increased until the pillar started to shed load. The pillar strength was defined as the peak vertical load, divided by the horizontal cross-sectional area of the pillar. The selected input parameters resulted in pillar strength of 48 MPa for a square pillar with W:H=1.0, which is 40% of the intact rock strength of 120 MPa used in the models. The model shows good agreement with the

empirical equation of Hedley and Grant (1972) for square pillars with W:H of 0.75 to 2.0.

Model results for pillar strength at the various stages of bench mining are presented in Figure 4, which shows how the pillar strength is progressively reduced as bench mining is carried out around the pillar. The model results show that strength of the pillar with W:H=1.0 is reduced by about 16%, from its initial value of 48 MPa to a final value of 40 MPa. The pillar with W:H=1.5 experiences a

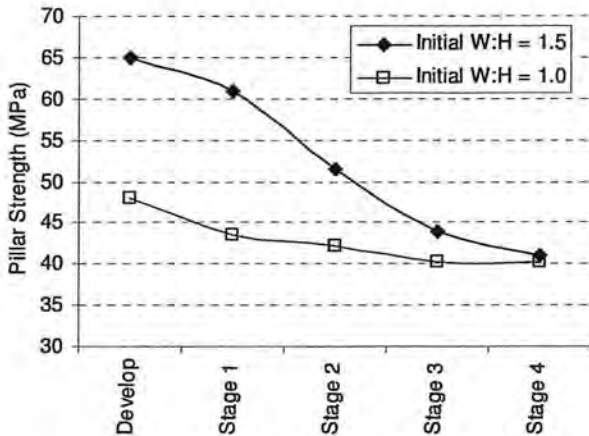


Figure 4. Results of FLAC3D modeling showing strength reduction of pillars with initial W:H=1.0 and 1.5 from initial development through various stages of bench mining. Final W:H ratios at Stage 4 are 0.5 and 0.75 respectively.

reduction in strength of 37% from the development stage to the fully benched stage.

From a pillar design point of view, it is important to also know how bench mining affects the pillar loads while the strength reduction is occurring. This aspect was assessed using numerical models and is discussed below.

### 3.2 Analysis of Changes in Pillar Loading During Benching

The examine 3D (Anon, 1998) boundary element package was used to determine how the pillar load is likely to change in response to benching. The program allows an array of pillars to be modeled in three dimensions assuming elastic rock properties. Benching of the floor can be modeled realistically and deflection of the roof over the benched and development pillars is simulated.

The rock mass was modeled with a Young's modulus of 30 GPa, to account for rock mass discontinuities, and Poisson's ratio of 0.2. The field stresses were set up to simulate a horizontal to vertical stress ratio of 2.0 at a depth of 200 m. The models simulated an array of pillars each 12 m wide and having W:H ratios of 1.0. The floor of the model was removed in stages to simulate benching to W:H of 0.5. The rooms were equal in width to the pillars, resulting in 75% extraction of the modeled

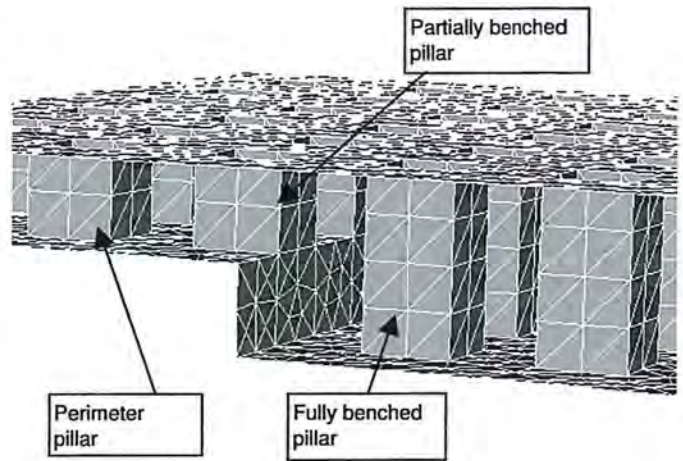


Figure 5. Cutaway view of Examine 3D model showing development and benched pillars.

limestone. Figure 5 shows a cut-away view of the model in which the initial developed pillars, the perimeter pillars and the benched pillars can be seen.

Figure 6 shows the average stress in the pillars obtained from a model in which half of the pillars have been benched. The results show that the development pillars at the edge of the benched area are subjected an increase of about 12% in their average stress. The results further show that the stress in the partly benched pillar is lower than the stress in the adjacent pillar that has not been benched yet, indicated as "perimeter pillar" in Figures 5 and 6. The lower stress in the partly benched pillar can be explained by the fact that its stiffness is reduced by the increase in height of one of the sides of the pillar, causing the load to be transferred to the stiffer development pillars. It can clearly be seen that the fully benched pillars are at a reduced stress level, owing to their relatively low stiffness. As benching continues, the stress in the fully benched pillars is expected to gradually

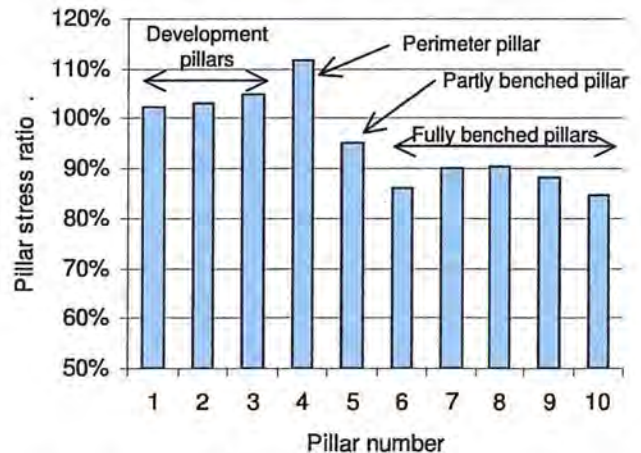


Figure 6. Results of Examine 3D model showing the average pillar stress during bench mining as a ratio of the average pillar stress prior to bench mining.

increase back to the tributary stress.

Further results, showing the changes in the average vertical stress in a pillar at the various stages of bench mining are presented in Figure 7. The figure also shows the associated changes in the pillar strength for a pillar with  $W:H=1.5$ , as previously presented in Figure 4. It can be seen that the pillar stress is a maximum just before benching starts around the pillar. As soon as one side of the pillar has been benched, the average pillar stress decreases, owing to the increased height and reduced stiffness. The average pillar stress continues to decrease as benching progresses, until the pillar is fully benched. The stress in the fully benched pillars will gradually rise as the benching face moves away. Full tributary loading can re-establish in the benched pillars if the mined area is sufficiently large.

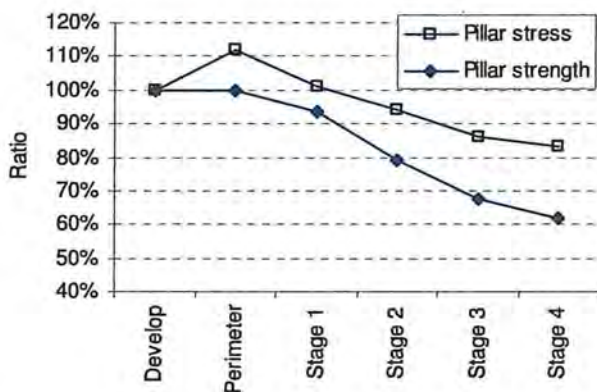


Figure 7. Change in the average vertical pillar stress and strength during various stages of bench mining, for a pillar with  $W:H=1.5$  based on FLAC3D and Examine3D results.

These results indicate that bench mining activities will result in an increase in the pillar stress around the perimeter of the benched area. However, once the pillar is partially benched, the average pillar stress will decrease.

### 3.3 Stress Concentration and Damage

The numerical models confirm that elevated stresses can occur in pillars around the perimeter of a benched area. However, the existence of reduced stresses in the partially benched pillars seems to be in conflict with the field observations, which indicate that elevated stresses exist in the partially benched pillars. Nearer inspection of the model results show that stresses are not symmetrically distributed within pillars at the edge of a benched area, shown in Figure 8. It can be seen that zones of high stress exist within the partially benched pillar that are absent in the perimeter pillar, although the average vertical stress in the two pillars may be similar. The elevated local stresses are likely to

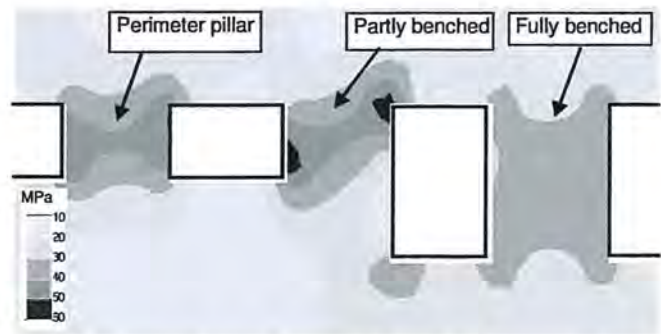


Figure 8. Section through the central part of an Examine 3D model showing maximum principal stress contours in and around pillars at the edge of bench mining. Contours in MPa.

contribute to the failure observed in the partially benched pillars in operating mines.

## 4 CASE STUDY OF BENCHING-RELATED INSTABILITY

### 4.1 Observed Instability

Pillar instability was observed adjacent to an area of bench mining at a mine that is extracting a near horizontal limestone bed. Spalling of the pillar ribs, resulting in hourglass formation, was observed. In the area of concern, the pillars were square with side dimensions varying between about 12.2 and 15.2 m and were initially benched to 15.8 m high. Further benching was carried out, which increased the pillar height to 27 m. The room width was measured to be about 16.4 m, and the depth of cover is 140 m. The average pillar stress is about 15 MPa, based on the tributary area method. However, the irregular pillar shapes and effects of benching resulted in variable stresses in the pillars. The width to height ratio of the benched pillars was as low as 0.44 in the 27 m high area. Figure 9 shows a plan of the mine

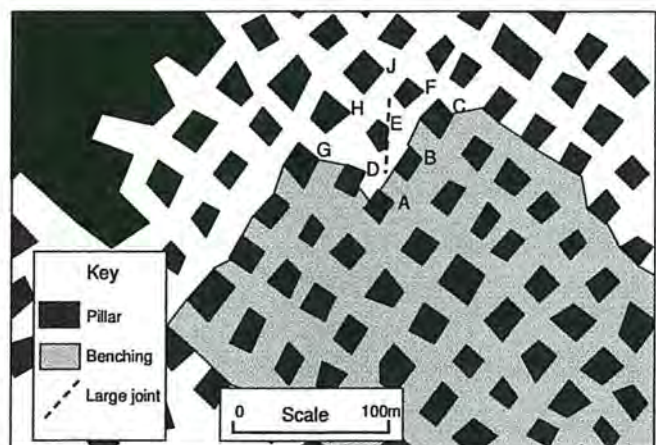


Figure 9. Plan view showing layout of pillars and bench mining at case study mine as modeled using the Examine 3D software.

workings indicating the area in which benching was carried out to a height of 27 m.

The limestone formation in this mine has uniaxial compressive strength in the range of 200-250 MPa. Jointing is near vertical with an average spacing of about 50 cm. A survey of joint orientations in the area showed that the main joint set strikes in the North-South direction. A single large, near vertical joint, was observed in the roof adjacent to Pillar E, and is shown Figure 9. Joint surfaces are rough, and the joint continuity is less than 3 m. Bedding joints are poorly developed and did not appear to affect the pillar stability. The rock mass rating (RMR) for this area was determined to be 78 as shown in table 4.

Table 4. Rock Mass Rating parameters in vicinity of unstable pillars at case study mine.

Parameter	Value	Rating
Intact rock strength	150 MPa	14
Joint frequency	2.0 joints/m	21
Joint condition	Rough joints with no infill, poorly developed bedding, joint walls unaltered	28
Groundwater	Dry	15
<b>Total:</b>		<b>78</b>

The initial development mining was carried out about 15 years ago, but the final benching stage was carried out less than 5 years ago. A number of pillars were reported to be progressively spalling to the current hourglass shape at the perimeter of the benched area. Figure 10 shows the conditions of pillars B and E. Evidence of fracture through intact rock and slab formation was seen. Pillars A, B, D and E showed open vertical fractures and there were large slabs lying on the mine floor around the pillars. Pillar E was considerably reduced in size, owing to the presence of the large joint that intersected one of its corners and caused the corner to slough. The remaining part of the pillar was in a poor condition, containing many stress related fractures and slabs. Pillars C, F, H and J were in a relatively good



Figure 10. View of pillars showing slabbing and rubble from rib failure, Pillar B on left and Pillar E on right in photograph.

condition and did not show any signs of stress damage.

#### 4.2 Analysis and Discussion

The pillars labeled A, B, D and E in Figure 10 are clearly exposed to elevated loading. Spalling to an hourglass shape, open fractures and slab formation are all well known manifestations of pillar overload. A 3D model of the area was set up using the Examine 3D software. The model simulated an area of about 300x300m with the pillars in question located near the center of the model. Two stages were modeled. The first stage simulated a condition prior to bench mining and the second simulated the benched configuration shown in Figure 9. The results showed that prior to bench mining, pillars D, E and F were slightly more stressed than the surrounding pillars owing to their smaller size. The stress distribution in the pillars after benching is shown in Figure 11. It can be seen that pillars D, E and F contain the highest stresses and A, B and C have already been partly relieved of stress by the bench mining. Pillar E carries the highest stress, because it is smaller than the other pillars, and is stiffer than the partially benched pillars. The relatively lower stresses in pillars A, B and C is expected, since their height has been increased by benching, and they have shed stress. However, as benching approached these pillars, the stresses will have been elevated and is likely to have caused the observed damage. The benching configuration, which forms a protruding right-angle, also contributes to the elevated stresses on these pillars.

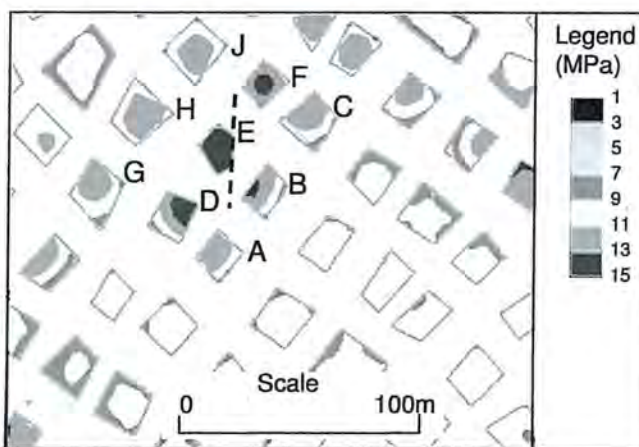


Figure 11. Examine 3D results showing contours of maximum principal stress in the pillars.

## 5 SUMMARY AND CONCLUSIONS

Observations show that floor benching can cause instability of pillars at the perimeter of bench mining operations. Instabilities can be caused by the

geological structures in the rock and by an increase in pillar loading.

The presence of large inclined joints or other geological discontinuities can cause instability because they are more likely to be exposed by the increased height of pillars.

An increase in pillar loading can be explained by considering the pillar stiffness. The benched pillars have a reduced stiffness and will shed load onto the stiffer development pillars. The numerical models showed that there was an increase in stress of about 15% in the pillars around the perimeter of the benching operations.

The models also showed that the strength of a pillar is reduced in a near linear manner as each side of the pillar is bench mined. The net effect is that partly benched pillars experience a simultaneous reduction in strength and load.

The instability of the partly benched pillar can be further ascribed to the uneven distribution of stresses within the pillars when they are located at the edge of a benching operation. High local stresses near the top and bottom of the pillar can initiate stress spalling.

The case study confirmed that increased stresses exist within pillars at the perimeter of the bench mining operations. It was further shown that irregular sized pillars are more likely to become unstable during bench mining. The smaller pillars are more susceptible to stress increases as benching approaches. The case study also showed that the benching should advance in a straight line, to avoid lagging corners that will result in elevated stresses in the perimeter pillars and degrade their stability.

## 6 REFERENCES

1. Anon. 1998. *Examine3D, User's Manual Version 4.0*, Toronto, Canada: Rockscience, Inc.
2. Anon. 2005. *FLAC 3D, Fast Lagrangian Analysis of Continua, User's Manual Version 3.0*. Minneapolis, Minnesota: Itasca Consulting Group
3. Bieniawski, Z.T. 1989. *Engineering Rock Mass Classifications*. New York: Wiley.
4. Diederichs, M.S. 2002. Stress induced damage accumulation and implications for hard rock engineering. Hammah Et Al. (eds.), *NARMS-TAC 2002*:3-12. University of Toronto.
5. Diederichs, M.S., Coulson, A., Falmagne, V., Rizkalla, N. & Simser, B. 2002. Application of rock damage limits to pillar analysis at Brunswick Mine Hammah Et Al. (eds.), *NARMS-TAC 2002*:1325-1332. University of Toronto.
6. Esterhuizen, G.S., Iannacchione, A.T., Dolinar, D.R. & Ellenberger, J.L. 2006. Pillar stability issues based on a survey of pillar performance in underground limestone mines. Peng SS, Mark C, Finfinger GL, Tadolini SC, Khair AW, Heasley KA, Luo Y, (eds). *Proceedings of the 25<sup>th</sup> International Ground Control Conference, Morgantown, WV*, 1-3 August 2006. pp. 354-361.
7. Esterhuizen, G.S. 2006. The strength of slender pillars. *Society for Mining Metallurgy and Exploration Annual Meeting, Preprint 06-003*. St. Louis, MO, March 2006.
8. Hedley, D.G.F. & Grant, F. 1972. Stope and pillar design for the Elliot Lake uranium mines. *Can. Inst. Min. Metall. Bull* 65:37-44.
9. Hoek, E. & Brown, E.T. 1997. Practical estimates of rock mass strength. *Int. J. Rock Mech. & Min. Sci. & Geomech.*, Abstr. 34:1165-1186.
10. Kaiser, P.K., Diederichs, M.S, Martin, D.C. & Steiner, W. 2000. Underground works in hard rock tunneling and mining. Keynote Lecture, *Geoeng2000*:841-926. Melbourne, Australia: Technomic Publishing Co.
11. Martin, C.D. & Maybee, W.G. 2000. The strength of hard rock pillars. *Int. Jnl. Rock Mechanics and Min. Sci.* 37:1239-1246.
12. Mine Safety & Health Administration. 2006. Web page: [www.msha.gov/stats](http://www.msha.gov/stats).